Med. **142**, 1283 (1982).
20. H. H. Samuels, F. Stanley, L. E. Shapiro, *Proc. Natl. Acad. Sci. U.S.A.* **73**, 3877 (1976).
21. ——, *J. Biol. Chem.* **252**, 6052 (1977).
22. F. Sanger, S. Nicklen, A. R. Coulson, *Proc. Natl. Acad. Sci. U.S.A.* **74**, 5463 (1977).
23. G. Chamness and W. McGuire, *Steroids* **26**, 538 (1975).
24. J. M. Chirgwin, A. E. Przybla, R. J. MacDonald, W. J. Rutter, *Biochemistry* **18**, 5294 (1980).
25. T. Maniatis, E. F. Fritsch, J. Sambrook, *Molecular Cloning: A Laboratory Manual* (Cold Spring Harbor Laboratory, Cold Spring Harbor, NY, 1982).
26. H. H. Samuels, F. Stanley, J. Casanova, *Endocrinology* **105**, 80 (1979).
27. We thank H. F. Bunn and J. Majzoub for helpful discussions and S. Tribuna for assistance in preparing the manuscript.

30 August 1988; accepted 3 January 1989

Odor-Induced Membrane Currents in Vertebrate-Olfactory Receptor Neurons

STUART FIRESTEIN* AND FRANK WERBLIN

In olfactory receptor neurons, odor molecules cause a depolarization that leads to action potential generation. Underlying the depolarization is an ionic current that is the earliest electrical event in the transduction process. In two preparations, olfactory receptor neurons were voltage-clamped and stimulated with odors and this generator current was measured. In addition, a method was developed to estimate the time course and absolute concentration of odorants delivered to the receptor sites. With this method, olfactory neurons were found to have relatively high stimulus thresholds, steep dose-response relations, long latencies, and an apparent requirement for cooperativity at one or more steps in the pathway from odorant binding to activation of the generator current.

OLFACTORY TRANSDUCTION IS PRESUMED to be mediated by a membrane-bound receptor protein which is activated and initiates a multistep pathway leading to the generation of action potentials in the olfactory nerve (*1*). An early step in this process is the odorant-induced activation of a depolarizing generator current. Efforts directed toward measurement of this current have been unsuccessful because the small, inaccessible cells have been difficult to impale with microelectrodes. In addition, the indirect access of stimuli to the cells has created conditions in which stimulus parameters such as concentration and duration cannot be known with any surety (*2*). Recently the whole cell patch-clamp technique (*3*) has been applied to isolated olfactory receptor cells with some success, but the absence of a repeatable and enduring odorant response in otherwise healthy cells has been a common disappointment (*4*).

We suspected that the failure of these receptors to give an odor response might have been due to the action of proteolytic enzymes, such as papain, commonly used to isolate the cells from the epithelium (*4*). Accordingly, we developed a slice preparation (*6*) (Fig. 1) that required no enzymatic treatment and left the tissue relatively intact while exposing cells sufficiently to provide access for the patch electrode (*5*).

Because the cells in the slice could respond to odors, we also tried isolating cells from the epithelium by mechanical means that did not require the use of enzymes. With care, viable cells could be isolated and odor responses that were identical to those seen in slice cells were obtained. In approximately 70% of the cells tested, a gigohm seal was attained and successful whole cell recordings obtained. Of these cells nearly 66% showed a response to the odor solution. The only consistent bias in the choice of cells was that cilia be present. There was no difference in the success rate between isolated cells and those in the slice; the results presented here are from cells prepared both ways.

The stimulus was an odorant "cocktail" consisting of acetophenone, amyl acetate, cineole, phenylethylamine, and triethylamine. Saturated aqueous stock solutions of each odorant were prepared in distilled water with a separatory funnel. We could then calculate the molar concentration of each saturated solution from the aqueous saturation coefficients (*7*). These solutions were diluted to 10^{-3} or $10^{-4}M$ with salt solutions that brought the osmolarity to that of the normal Ringer solution. All solutions were brought to *p*H 7.6 with NaOH. Thus the cocktail contained millimolar or 0.1 millimolar concentrations of each of the five odorants in an osmotically balanced Ringer solution.

The current-voltage (*I-V*) relation for the generator current (Fig. 2) was obtained by holding the membrane at potentials from −70 mV to +30 mV and pressure ejecting an odorant pulse (*8*). The current was linear with membrane potential throughout the physiological range and reversed near +5 mV, suggesting that it is a nonspecific cation conductance. The adenosine 3′,5′-monophosphate (cAMP)–activated conductance in ciliary membrane patches shows a similar *I-V* relation (*9*), and the macroscopic current elicited by cAMP application is carried by Na^+, K^+, and Ca^{2+} (*10*).

Odor responses were rarely seen if the concentration of the odorant mixture in the delivery pipette was less than $10^{-3}M$. Initially this seemed high, but with the pressure-ejection delivery system it was impossible to calculate, from pulse duration and pressure alone, the absolute concentration of stimuli reaching the ciliary membrane.

We developed a method of measuring the magnitude of applied odorant at the cilia on the basis of the K^+ permeability of the cell. A stimulus of the odorant cocktail in an elevated (with respect to Ringer solution) K^+ solution was ejected at the cell (Fig 3). An inward current appeared in response to the transient elevation of K^+ and the magnitude of this current was used as a measure of the K^+ concentration reaching the cell (*11*). This value could be used to determine the absolute concentration of odorant at the cell membrane in the following way (*12*). Knowing the concentration of K^+ in the pipette and the concentration arriving at the cell, we were able to determine the fraction of K^+ that reached the cell (K_{frac}) for a given pressure pulse:

$$K_{frac} = [K]_{cell}/[K]_{pipette}$$

where the subscripts cell and pipette mean "at the cell" and "in the delivery pipette," respectively. Because the odorants were mixed to a known concentration in the same pipette solution and the fraction of odorant reaching the cell ($[O]_{cell}$) was the same as K_{frac}, it follows that:

$$[O]_{cell} = K_{frac}\,[O]_{pipette}$$

The subscripts have the same meaning as above.

We took advantage of the finding (Fig. 3) that the change in clamp current to changes in K^+ concentration around the cell was nearly instantaneous, but the onset of the response to odorant was delayed (by the transduction process) by more than 100 ms. Thus the two currents could be measured independently.

Knowing the absolute value of the odor-

Graduate Group in Neurobiology, 275 Cory Hall, University of California at Berkeley, Berkeley, CA 94720.

*To whom all correspondence should be addressed at Section of Neuroanatomy, Yale School of Medicine, 333 Cedar Street, New Haven, CT 06510.

ant concentration at the cilia allowed us to construct dose-response curves (Fig. 3B). For six cells, the curves shifted along the concentration axis over an order of magnitude but their shape remained constant. The lowest concentration at which we could detect a measurable response was 6 μM. The mean $K_{1/2}$ (the concentration of odorant that elicited the half-maximal response) for six cells was $2.80 \times 10^{-5} M$ (SD = 1.44×10^{-5}). The cell in the figure had a somewhat higher threshold at $1.66 \times 10^{-5} M$ and a $K_{1/2} = 5.01 \times 10^{-5} M$. This variability may reflect differing sensitivities or different classes of cells. A similar range in the respone of ciliary patches to cAMP has been reported (*9*).

The sigmoidal shape of both the dose-response curve and the individual responses suggested that there is a cooperative process in the chain of events from odorant binding to ion channel activation. The presence of a ciliary-specific adenylate cyclase that is activated by odorants (*13*) and of cAMP-dependent ion channels in patches of ciliary membrane (*9*) implicate a second messenger system. The adenylate cyclase step has a Hill coefficient of less than 1, and the cAMP activation of the ion channel has a Hill coefficient of 1.6 (*9, 13*). Plotting our data on Hill coordinates and fitting the points with a straight line, we measured a Hill coefficient, n_{app}, of 2.7 (Fig. 4). Because we are examining a multistep process, it is impossible to deduce a precise physiological mechanism from this number, but it does provide further evidence that cooperativity is important at one or more steps in the transduction pathway.

In addition to allowing us to estimate the odorant concentration at the cilia, the K^+ response also provided temporal information about the stimulus. The time course of the response to K^+ indicates the time course of the arrival of the ejected solution, including both K^+ ions and odor molecules, at the cell membrane. In contrast with previous studies (*14*), there is no mucus in this preparation nor is there any air-water phase boundary through which the odorant molecules must partition for access to receptors. Both of these conditions normally present incalculable barriers that have confounded both magnitude and temporal measurements.

The response to K^+ appeared within 20 ms of the pressure pulse, probably coincident with the arrival of the solution at the membrane, and the entire K^+ response was virtually completed before the odor-induced generator current activated. The generator current appeared after a latency of 140 to 570 ms (mean, 320 ms; *n*, 19), as measured from the onset of the K^+ current. This latency was only slightly concentration-dependent, becoming shorter at higher concentrations, but was never less than 140 ms. Because they are measured from the arrival of the stimulus at the membrane surface, these latencies are entirely due to cellular processes; they are not a property of the mucus or other access barriers (*2*). The long latency lends further support to the existence of a second messenger enzyme cascade (*9, 13, 15*) and makes it less likely that the ion channel is directly gated by the odorant molecule (*16*).

We have reported our data here as responses to the peak stimulus concentration. Although this is in keeping with common practice, it may not be appropriate in all cases. Olfactory receptors could be responding to the maximum concentration in a dose-dependent manner or they could be integrating stimulus flux over some time period, that is, "counting" molecules much as photoreceptors count photons (*17*). We have found that for short pulses less than 100 ms the shape of the dose-response curves was unchanged whether peak or integrated concentration values were plotted. This is different than the behavior of photoreceptors in their responses to flashes and steps of light (*17*). However, for longer pulses (200 to 400 ms) the responses more closely followed the integral of the stimulus intensity and not the peak. Indeed we have

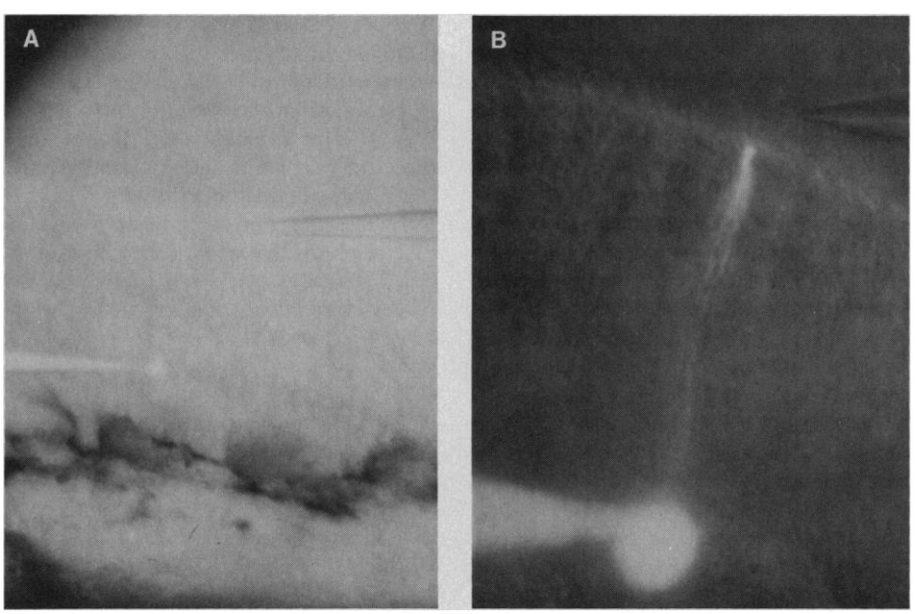

Fig. 1. Photomicrograph of olfactory receptor in a slice of epithelium taken from a terrestrial phase salamander, *Ambystoma tigrinum*. The slice is prepared by a method similar to that developed for the retina by Werblin (*19*). Briefly, a small (3 mm by 3 mm) piece of epithelium is dissected free of the underlying cartilage and laid, mucus side up, on a piece of Millipore filter. The tissue adheres tenaciously to the filter even when submerged in a bath of Ringer solution. Using a microtome blade on a flexible arm, we sliced the tissue and filter into approximately 150- to 200-μm-thick slices. These strips of tissue and filter are turned 90° and held in two parallel Vaseline tracks, presenting a cross section of living epithelium. This permits access to cells on the surface of the slice by the patch pipette and access to the cilia by a pressure-ejection glass pipette. The slice affords a clear visualization of the anatomic structures described for fixed epithelium (*20*). The patch electrode solution contained 1% Lucifer yellow CH (Sigma), which completely dialyzed the cell interior, including the cilia, within 2 min. (**A**) Objective, ×20; total magnification, ×200; the stimulus-containing pipette can be seen near the top of the slice; (**B**) ×40 water immersion objective (Zeiss) with 1.6-mm working distance and Hoffman modulation contrast optics; total magnification, ×400. (A) and (B) are the same cell. The ejection pipette is at top right, placed within 30 μm of the cilia. The cell soma is out of the plane of focus.

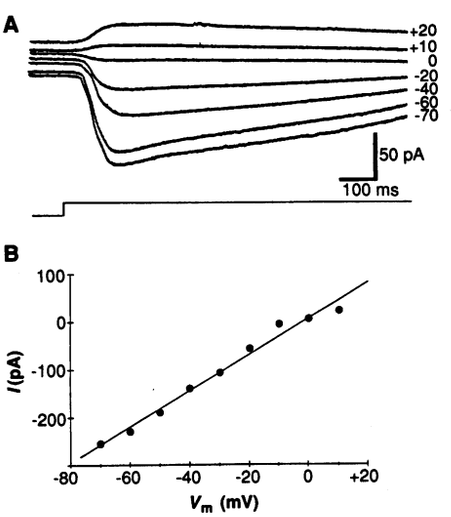

Fig. 2. (**A**) A series of responses to 1-s-long odorant puffs delivered once every minute while the membrane potential was varied from −70 mV to +20 mV. CsCl replaced KCl in the electrode. Data were recorded from a cell in a slice. (**B**) *I-V* relation for cell in (A).

seen cells that appeared to have no odor response when tested with short pulses, but responded to longer pulses, even though the peak concentration attained during each pulse was the same. There is considerable variability in this behavior and we are currently unable to offer a quantitative description. Here we have used peak concentration values since all the experiments were conducted with short pulses and have reported responses to peak values in molar units (as opposed to integrated units of moles per second) to facilitate comparison with earlier data. However, we believe that responses to longer stimulus presentations must take the integration factor into account.

From this analysis some insights into olfactory transduction are possible. Olfactory receptor neurons responded with measurable currents to odorants in the micromolar or higher concentration range. Reports of responses to concentrations lower than this are from preparations in which the mucus layer is intact and odorants are presented in the vapor phase for pulses lasting one to several seconds (*14*). The mucus and the length of the pulse might serve to concentrate the odor molecules near the receptors (*2*). Furthermore, the air-mucus partition coefficients favor absorption of odorants into the mucus compartment (*18*). Activation of a ciliary adenylate cyclase by odorants in vitro has indicated a similarly high $K_{1/2}$ value (*13*).

The dynamic range of the typical olfactory receptor seems limited. The dose-response curves are steep, saturating over less than a log unit of concentration change. This is consistent with extracellular recordings in which firing frequencies vary from 0 to a maximum of 20 to 25 spikes per second over a similarly narrow concentration range (*14*).

Finally, a response latency of several hundred milliseconds lends support to the hypothesized second messenger system. Although the delay could arise from the direct gating of the conductance by a membrane receptor requiring binding of several ligand molecules for activation, the latencies recorded here seem too long, even if all of the observed cooperativity in the dose-response relation is attributed to the receptor protein. For example, currents directly gated by nicotinic acetylcholine receptors activate with latencies on the order of 1 to 10 ms, more than an order of magnitude faster than the odor-induced current (*16*). Also, the sigmoidal rise of the current requires a kinetic scheme more complex than could be attributed to a model in which all the parameters resulted from receptor-ligand binding cooperativity (*16*). Rather, these currents share more features with those underlying slow synaptic potentials or photoreceptor responses, both of which are the result of second messenger action (*16, 17*).

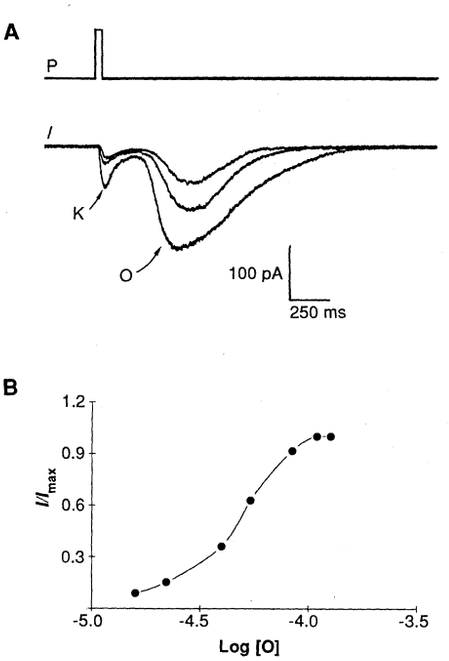

Fig. 3. (**A**) A series of responses to puffs of $10^{-3}M$ odorant cocktail and 100 mM K^+ mixed as a single solution and ejected from the same pipette. The initial inward current deflection (K) is the K^+ response followed by the larger, slower generator current (O). These responses were elicited by pressure steps of 1, 2, and 4.5 psi lasting 50 ms each. Upper trace is a record of the solenoid-valve operation, the actual time course of the stimulus is more closely reflected by the K^+ current. (**B**) Dose-response relation for a typical cell. The sigmoidal rise is steeper than that predicted by a Michaelis-Menten type equation.

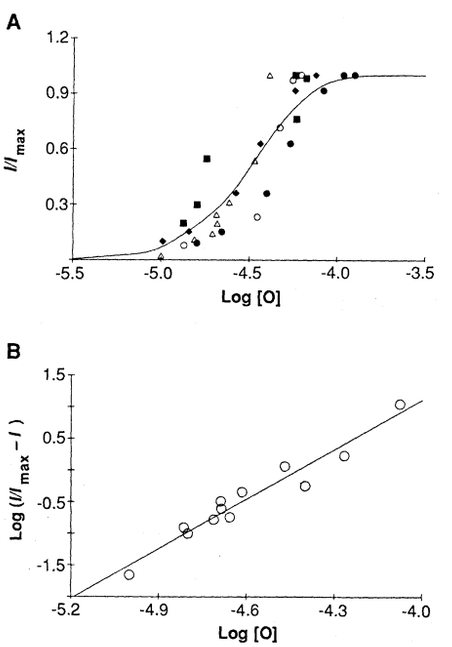

Fig. 4. (**A**) Pooled data from five cells. The solid curve was fitted by an equation of the form $B = 1 - \exp(-xn)$, where B is the normalized response, x is the relative concentration of odorant, and n is a proportionality constant characteristic of each cell and may be related to the degree of cooperativity. For these data the mean (n) was equal to 2.7. (**B**) Hill plot for data from two of the cells in (A); (◆) and (●) were selected to cover the widest range of odorant concentrations. Log $\{I/(I_{max} - I)\}$ is plotted as a function of log [O], where I is the current amplitude and O is the odorant concentration. Straight line is a best fit by least-squares method; slope is the Hill coefficient, $n_{app} = 2.7$ (± 0.2 SEM), which is the same as n in (A).

REFERENCES AND NOTES

1. D. Lancet, *Annu. Rev. Neurosci.* **9**, 329 (1986).
2. T. V. Getchell, F. L. Margolis, M. L. Getchell, *Progr. Neurobiol.* **23**, 317 (1984).
3. O. P. Hamill, A. Marty, E. Neher, B. Sakmann, F. J. Sigworth, *Pfluegers Arch.* **391**, 85 (1981).
4. S. Firestein and F. S. Werblin, *Proc. Natl. Acad. Sci. U.S.A.* **84**, 6292 (1987); V. E. Dionne, *Abstr. Ninth Int. Symp. Olfaction Taste* **S45** (1986); N. Suzuki, *ibid.* **S46** (1986); D. Trotier, *Pfluegers Arch.* **407**, 589 (1986); P. A. V. Anderson and K. A. Hamilton, *Neuroscience* **21**, 167 (1987).
5. Whole cell patch-clamp recordings were made with a DAGAN 8900 patch-clamp, and data were recorded directly to computer hard disk with software developed in our laboratory for the IBM XT computer. Electrodes were fabricated with a Sutter S30 electrode puller by means of a single pull with borosilicate glass of 1.5-mm outer diameter (WPI). Electrode resistance was 5 megohms. Series resistance was checked regularly during the course of an experiment to be sure it was always <10 megohms. Normal bathing solution contained 120 mM NaCl, 2.5 mM KCl, 4.0 mM $CaCl_2$, 0.4 mM $MgCl_2$, 5.0 mM Hepes, and 5.0 mM glucose, pH 7.6. The intracellular solution contained 125 mM KCl, 2.0 mM $MgCl_2$, 0.1 mM $BaCl_2$, 2.0 mM EGTA, 1.0 mM adenosine triphosphate (ATP), and 1.0 mM guanosine triphosphate (GTP), pH 7.6. For Lucifer yellow–filled electrodes the KCl was replaced with equimolar CsCl.
6. S. Firestein and F. S. Werblin, in *Transduction Mechanisms in Taste and Olfaction*, J. G. Brand, Ed. (Dekker, New York, in press).
7. M. Windholz, Ed., *The Merck Index* (Merck, Rahway, NJ, ed. 10, 1983); R. C. Weast, Ed., *Handbook of Chemistry and Physics* (CRC Press, Boca Raton, FL, ed. 69, 1988).
8. Pressure-ejection pipettes were fabricated from the same glass and in the same way as recording electrodes except that the lumens were at least 4 μm in diameter. A picospritzer (General Valve) was used to set pressure and duration parameters.
9. T. Nakamura and G. Gold, *Nature* **325**, 442 (1987).
10. N. Suzuki, *Chem. Senses* **13**, 311 (1988).
11. The concentration of potassium ions ([K^+]) at the cell that gave rise to the inward current seen in Fig. 3 was determined as follows: The peak of the K^+ current was related to the [K^+] by

$$i_K = g_K (E_2 - E_1)$$

where i_K is the current, g_K is the conductance, E is the membrane potential, and

$$E_2 - E_1 = 0.025 \ln(K_2/K_1)$$

with K_1 and K_2 equal to the initial (bath) and final (puff) [K^+], respectively. Therefore,

$$i_K = g_K\ 0.025 \ln(K_2/K_1)$$

The g_K was determined by applying a high pressure, long duration pulse that brought the [K] around the cell to the value in the pipette. This permitted us to calculate g_K for each cell from,

$$g_K = i_K/0.025 \ln(K_2/K_1)$$

Having a value for g_K, we could determine the puffed [K^+] at the cell from:

$$K_2 = K_1 \exp(i_K/g_K\ 0.025)$$

This is the fraction of the K^+ in the pipette that arrives at the cell.
12. For these experiments cells with short dendrites (<10 μm) were selected so that the cilia and soma

were within a spherical volume of radius <25 μm. The pipette was always positioned such that it was 20 to 25 μm from the dendritic knob and that the solution passed over the cilia before reaching somatic membrane. Since the distance from the cilia to the dendrite and soma was no more than 15 to 30 μm, the force of ejection was sufficient to cause the solution to arrive within fractions of a millisecond everywhere in the region of the cell. We included the dye fast green in the pipette and affirmed that the pulsed solution rapidly engulfed the entire cell. If the solution only partially surrounded the cell, our estimates for concentration would be low.
13. U. Pace, E. Hanski, Y. Salomon, D. Lancet, *Nature* **316**, 255 (1985); P. B. Sklar, R. R. H. Anholt, S. H. Snyder, *J. Biol. Chem.* **261**, 15538 (1986).
14. T. V. Getchell and G. M. Shepherd, *J. Physiol. (London)* **282**, 541 (1978).
15. T. Huque and R. C. Bruch, *Biochem. Biophys. Res. Comm.* **137**, 36 (1986).
16. P. Labarca *et al., Proc. Natl. Acad. Sci. U.S.A.* **85**, 944 (1987); J. S. Kehoe and A. Marty, *Ann. Rev. Biophys. Bioeng.* **9**, 437 (1980); H. C. Hartzell, S. W. Kuffler, R. Stickgold, D. Yoshikami, *J. Physiol. (London)* **271**, 817 (1977).
17. D. A. Baylor, A. L. Hodgkin, T. D. Lamb, *J. Physiol. (London)* **242**, 759 (1974).
18. J. E. Amoore and R. G. Buttery, *Chem. Senses Flavor* **3**, 57 (1978).
19. F. S. Werblin, *J. Physiol. (London)* **264**, 767 (1977).
20. J. A. Rafols and T. V. Getchell, *Anat. Rec.* **206**, 87 (1983).
21. We thank P. Lukasiewicz and G. Maguire for a critical reading of the manuscript, S. Eliasof for assistance in data analysis, B. Maple for many useful discussions, and G. Shepherd for a helpful critique. Supported in part by grants from the U.S. Public Health Service.

19 September 1988; accepted 29 December 1988

Enhanced Activity and Altered Specificity of Phospholipase A_2 by Deletion of a Surface Loop

OSCAR P. KUIPERS, MARJOLEIN M. G. M. THUNNISSEN, PIETER DE GEUS,* BAUKE W. DIJKSTRA, JAN DRENTH, HUBERTUS M. VERHEIJ, GERARD H. DE HAAS

Protein engineering and x-ray crystallography have been used to study the role of a surface loop that is present in pancreatic phospholipases but is absent in snake venom phospholipases. Removal of residues 62 to 66 from porcine pancreatic phospholipase A_2 does not change the binding constant for micelles significantly, but it improves catalytic activity up to 16 times on micellar (zwitterionic) lecithin substrates. In contrast, the decrease in activity on negatively charged substrates is greater than fourfold. A crystallographic study of the mutant enzyme shows that the region of the deletion has a well-defined structure that differs from the structure of the wild-type enzyme. No structural changes in the active site of the enzyme were detected.

THE LIPOLYTIC ENZYME PHOSPHOLIPASE A_2 (PLA_2) specifically cleaves the 2-acyl linkage of phosphoglycerides in a calcium-dependent reaction (*1*). Phospholipases occur both extracellularly and intracellularly. The extracellular PLA_2's from mammalian pancreas and from snake venom (*1, 2*), and also the mammalian intracellular PLA_2's (*3–5*), exhibit a high degree of sequence homology. A difference between snake venom PLA_2's and the pancreatic enzymes is that the former ones in general have higher turnover numbers and a greater affinity for phospholipid molecules aggregated in micelles than the pancreatic ones (*6, 7*). In the pancreas but not in snake venom the enzyme occurs as a precursor that is activated in the duodenal tract by the tryptic removal of a small activation peptide from the NH_2-terminus.

The x-ray analyses of several PLA_2's from pig, ox, and *Crotalus atrox* venom (*8, 9*) show that these enzymes are structurally similar (*10*). A comparison of the structures of active bovine PLA_2 and that of inactive bovine precursor (*11*) shows that in the active enzyme the NH_2-terminal helix and loop 62 to 72 are well defined, whereas in the precursor this latter loop and the first three residues of the NH_2-terminal α helix are mobile. Because pro-PLA_2, contrary to active phospholipase, does not bind to aggregates of zwitterionic phospholipids, it has been suggested that a low mobility of the NH_2-terminal helix and the surface loop are required for efficient binding (*12*). A similar immobilization of the substrate binding domain has also been observed for trypsin after activation of trypsinogen (*13*).

Lipolytic enzymes hydrolyze aggregated substrates such as micelles, vesicles, and liposomes at much higher velocities than monomeric substrate molecules. Hydrolysis of these aggregated phospholipids requires the binding of the enzyme to the lipid-water interface. After binding of the enzyme to the lipid aggregates, one single substrate molecule is thought to diffuse into the active site, where it is hydrolyzed. Many of the residues involved in the binding to aggregated phospholipids have been identified by chemical modification studies of phospholipases from many sources. On the basis of these studies, it has been concluded that the porcine enzyme residues Leu^2, Trp^3, Arg^6, Leu^{19}, Met^{20}, Leu^{31}, and Tyr^{69} are involved in the interaction of the enzyme with lipid-water interfaces (*2*). The three-dimensional (3-D) structures of the pancreatic phospholipases show that these residues are all located at one face of the molecule around the active site (*14*). From these observations it has been inferred that the binding site of the enzyme for aggregated substrates is an extended region around the entrance of the

Table 1. Kinetic properties of two native and one mutant PLA_2 enzymes acting on various substrates (*20*). Assays on monomeric diC6dithioPC were carried out in the presence of 100 m*M* $CaCl_2$, 100 m*M* NaCl, and 200 m*M* tris-HCl at *p*H 8.0 in a spectrophotometric assay at substrate concentrations not exceeding 0.8 m*M* (*23*). Assays on micelles were carried out in the presence of 1 m*M* sodium borate, 25 m*M* $CaCl_2$, and 100 m*M* NaCl at *p*H 8.0. The syntheses of these substrates and details of the kinetic analyses are in (*24*). The K_m values are based on the concentration of micelles after correction for the concentration of free monomers. The K_m values are apparent because more than one equilibrium is involved (*1*). Enzymes: Wild-type, porcine pancreatic PLA_2; Δ62–66, Δ62–66 PLA_2; *N. melanoleuca*, fraction DE-III from the venom of *N. melanoleuca* (*6*). Standard errors of all values were less than 10% of the reported value. ND, not determined.

Enzyme	Monomeric diC6dithioPC			Micelles							
				diC6PC		diC7PC		diC8PC		diC7GS	
	k_{cat} (s^{-1})	K_m (m*M*)	k_{cat}/K_m (s^{-1} M^{-1})	k_{cat} (s^{-1})	K_m (m*M*)	k_{cat} (s^{-1})	K_m (m*M*)	k_{cat} (s^{-1})	K_m (m*M*)	k_{cat} (s^{-1})	K_m (m*M*)
Wild type	0.62	0.7	890	5	14	25	3.7	410	3.2	45	ND*
Δ62–66	0.90	0.5	1790	80	8	240	1.9	980	1.9	10	ND*
N. melanoleuca	ND†	ND†	ND†	830	ND*	980	ND*	3490	ND*	1	ND*

*Because of the formation of lipid-protein aggregates below the critical micelle concentration, K_m values could not be obtained. †Monomers of zwitterionic substrates induced the formation of lipid-protein aggregates for this venom enzyme, so that no true data for monomers could be obtained.

O. P. Kuipers, P. de Geus, H. M. Verheij, G. H. de Haas, Department of Biochemistry, University of Utrecht, Center for Biomembranes and Lipid Enzymology, P.O. Box 80054, 3508 TB Utrecht, The Netherlands.
M. M. G. M. Thunnissen, B. W. Dijkstra, J. Drenth, Laboratory of Chemical Physics, University of Groningen, Nijenborgh 16, 9747 AG Groningen, The Netherlands.

*Present address: Plant Genetic Systems, J. Plateaustraat 22, B 9000 Gent, Belgium.